Superlattices and Microstructures, Vol. 30, No. 4, 2001
doi:10.1006/spmi.2001.1002
Available online at http://www.idealibrary.com on IDEAL®

Pressure effects on nanoprobe photoluminescence of quasi-zero-dimensional confinement quantum dots

KAZUNARI OZASA
The Institute of Physical and Chemical Research (RIKEN), 2-1 Hirosawa, Wako, Saitama 351-0198, Japan

SINTARO NOMURA
Institute of Physics, University of Tsukuba, 1-1-1 Tennoudai, Tsukuba 305-8571, Japan

YOSHINOBU AOYAGI
The Institute of Physical and Chemical Research (RIKEN), 2-1 Hirosawa, Wako, Saitama 351-0198, Japan

(Received 20 July 2001)

Nanoprobe near-field photoluminescence (PL) of InGaAs(P) dots with quasi-zero-dimensional (quasi-0D) confinement with various degrees of 0D/2D has been investigated by studying probe-induced pressure effects and probe-bias effects. Fine PL peaks of 0D confinement are superimposed on quantum well (QW) peaks for quasi-0D structures, which proves the coexistence of 0D and two-dimensional (2D) confinement in the same layer. Large blue shifts of approximately 100 meV were observed to occur with pressure increase for 0D fine PL peaks, but no shift was observed for the QW peak. The fine 0D peaks were eliminated by larger probe-induced pressures, which should be attributed to carrier diffusion rather than to Γ–X crossover in energy levels. The QW peak increased with the positive probe bias, while 0D fine PL peaks showed a smaller increase with red shifts up to 8–9 meV. The results obtained can be explained by the excitation of immobile excitons in 0D potentials to mobile carriers in the 2D (QW) layer.

Key words: InGaAs dot coupling, near-field photoluminescence, SNOM, NSOM, pressure dependence, CBE.

1. Introduction

There is emerging interest in memory devices and infrared detectors [1–4] which use quantum dots (QDs) as charge reservoirs [5–9]. The excitons confined in QDs in these applications are emitted into a two-dimensional (2D) conduction layer by external perturbations such as gate voltage or infrared photons. Usually, the QDs are fabricated by a strain-induced self-organization mechanism, and the 2D conduction layer is spatially separated from the QD layer. For example, modulation-doped GaAs/AlGaAs heterointerfaces for 2D conduction are placed 10–50 nm apart from an InAs/GaAs QD layer [4]. In this structure, electrons are excited from the QDs by infrared photons and transferred into the GaAs/AlGaAs 2D interfaces by a built-in electric field. On the other hand, there are possibilities to use quasi-0D confinement structures with an intermediate confinement between 0D and 2D to realize 0D charge-reservoirs coexisting with a 2D conduction

0749–6036/01/100169 + 11 $35.00/0

layer in one plane. With such a quasi-0D confinement, one can expect that the carrier density and mobility in the 2D layer are affected more sensitively by the existence of charges in the 0D exciton reservoirs than in the case of spatially separated 0D–2D structures. To elucidate the realization of quasi-0D devices, it is necessary to fabricate the quasi-0D confinement structures and evaluate 0D/2D charge transition due to external perturbations.

Recently, we have succeeded in fabricating quasi-0D confinement structures of InGaAs(P)/GaAs by *in situ* phosphidation in a chemical beam epitaxy (CBE) chamber [10–12]. Here, *in situ* phosphidation is the process of exposing strain-induced InGaAs/GaAs dots to phosphorus flux at an elevated temperature to replace arsenic atoms in InGaAs dots with phosphorus atoms. The phosphidation causes the composition change of InGaAs $\rightarrow$ InGaAsP, and as a result, the dots are flattened due to strain relaxation, since the lattice parameter of the dots becomes close to that of GaAs. At the same time, the energy-gap bottom of the dots is pushed up to change the 0D confinement in the dots into a 2D confinement in a quantum well (QW). By controlling the phosphidation time (how long the InGaAs dots are exposed to the phosphorus flux), the fabrication of quasi-0D confinement structures with various degrees of 0D/2D is realized for the first time. Indeed, the intermediate characteristics between QDs and QWs were revealed in the temperature dependence of the macroscopic photoluminescence (PL) of the fabricated quasi-0D confinement structures [13]. In order to clarify the carrier transfer from 0D to 2D confinement by the external perturbation, however, more detailed study on the microscopic photoluminescence must be carried out.

In this report, we present a study on the low-temperature near-field PL of quasi-0D confinement structures measured using a scanning near-field optical microscope (SNOM), together with the PL dependence on uniaxial pressure and external electric field. The coexistence of 0D and 2D confinement was observed in a series of near-field PL spectra for structures with various degrees of 0D to 2D transition. The fine peaks originating from 0D confinements showed strong dependence on the uniaxial pressure applied by the SNOM probe itself; a blue shift of more than 100 meV occurred due to the pressure. The peaks increased and red shifted with an external electric field applied by probe-bias. In contrast, a rather broad PL peak originating from the coexisting QW was not affected by the probe-induced pressure, but increased markedly with positive probe-bias. These results indicate that the immobile excitons in 0D confinements in quasi-0D structures are transferable to the coexisting 2D conduction layer as mobile carriers as in conventional 2D electron gas (2DEG).

2. Experiment

The fabrication of quasi-0D structures was carried out in the following three steps: formation of InGaAs QDs by self-assembly, *in situ* phosphidation to partly flatten the dots, and subsequent GaAs capping growth. The entire fabrication process was performed in one CBE chamber, using triethylgallium (TEGa), trimethylindium (TMIn), precracked AsH_3, and precracked PH_3 as sources. The substrates used were semi-insulating GaAs (001). First, $In_{0.52}Ga_{0.48}As$ dots were prepared at 480 °C on a GaAs buffer layer (180 nm) based on the strain-induced self-assembly mechanism. The typical height, diameter, and density of these InGaAs QDs were 8.0 nm, 26 ± 5 nm, and $5-6\times10^{10}$ cm^{-2}, respectively, measured by separate experiments. Second, the InGaAs dots were exposed to phosphorus flux *in situ* at 480 °C for 0–90 s. The temporal change of dot composition and height is given in Fig. 1, which was obtained not by PL measurement but by *in situ* monitoring by reflection high-energy electron diffraction (RHEED). The dot composition can be calculated from the distance between the spots in RHEED patterns. The dot height was estimated through the linearly interpolated relation between RHEED spot intensity and QD height observed using an atomic force microscope (AFM). In separate AFM observation, a residual undulation of 1.3 nm height was obtained for 15 min-phosphidated samples. With regard to the diameter of the dots, we have found by SEM observation that the dots undergoing the flattening process are reduced in height rather than diameter until they coalesce into a layer. Several typical degrees of phosphidation were selected for near-field PL investigation, and are indicated in Fig. 1

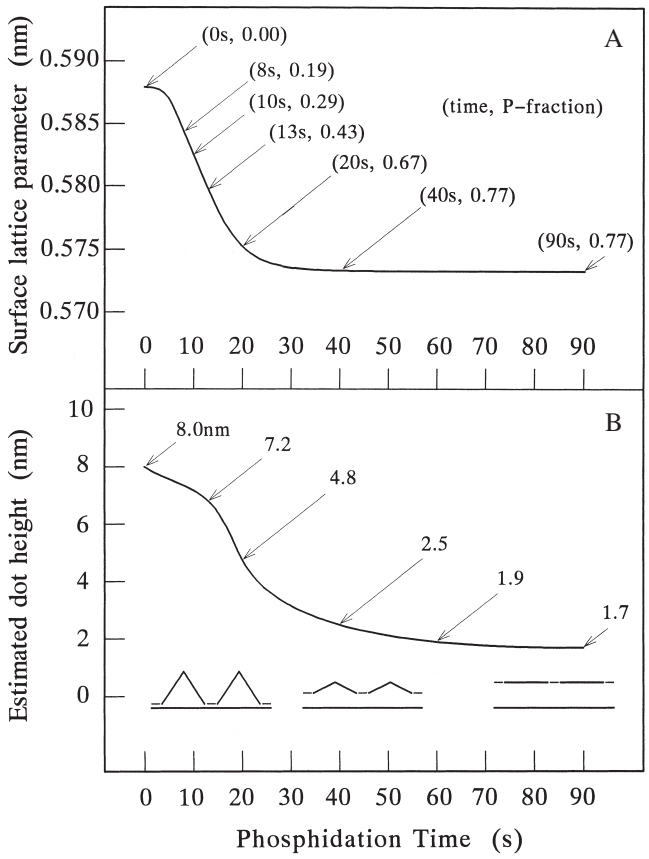

Fig. 1. Temporal change of surface lattice parameter and dot height, caused by the phosphidation of InGaAs dots [13]. The curve was obtained through *in situ* RHEED observation during phosphidation.

by arrows. Lastly, the quasi-0D structures were buried in 50 nm-thick GaAs by subsequent GaAs growth at 480 °C. All the structures prepared were not intentionally doped. Details of the preparation of the quasi-0D structures were reported in references [10–12].

Near-field PL measurements were performed with a liquid-He-cooled scanning tunnelling microscope (STM; Unisoku, USM-100R) equipped with an optical fibre system with an Au-coated fibre probe at the sample-side end (Fig. 2). The sample temperature measured by a thermocouple placed near the sample holder was typically 10 K. As shown in Fig. 2, a so-called collection mode was employed, that is, signal detection through the probe aperture with large-area excitation around the probe. The excitation was realized by a SHG–YAG laser (532 nm) at an incident power density of 540 mW cm^{-2} with 45° incidence. The luminescence was detected through a fibre probe with a small nominal aperture (approximately 2–3 μm), and led to a 0.3 m monochromator (Spex, 270 M) equipped with a liquid-N_2-cooled CCD detector (SPEX, CCD-2000). The resolution of our near-field PL system was approximately 0.5 meV. The fibre probe was operated by the conventional tunnel-current feedback control. After the probe was positioned on the sample surface, the feedback control was terminated to ensure that the position of the probe was fixed. Since the surface beneath the probe was shadowed by the probe itself, the luminescence was caused by the diffusion of photocarriers generated outside of the probe shadow.

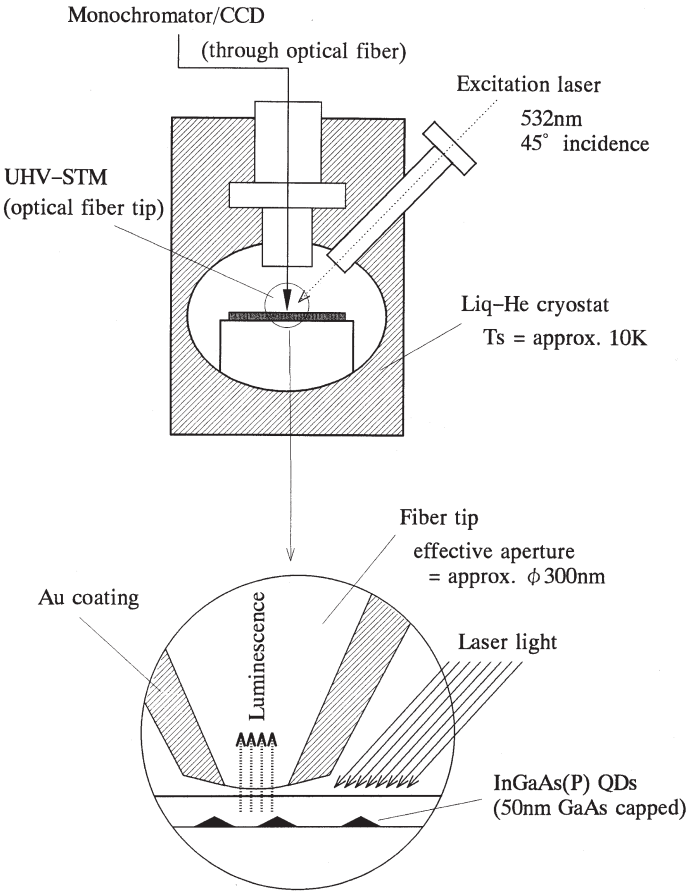

Fig. 2. Schematic diagram of nanoprobe PL measurements with a liquid-He-cooled STM. An optical fibre with an Au-coated fibre probe was used to detect the luminescence, while laser excitation was realized through an optical window.

3. Results and discussion

3.1. Near-field PL spectrum of quasi-0D structures

The phosphidation causes changes in the energy gap, size/strain distribution, and transition of 0D $\rightarrow$ 2D confinement. In order to observe the transition of 0D $\rightarrow$ 2D with phosphidation, we measured a series of near-field PL spectra for quasi-0D structures, where the coexistence of 0D and 2D confinement has been confirmed by fine PL structures originating from 0D superimposed on a QW peak for 20 and 90 s-phosphidated structures.

Figure 3 shows the near-field PL spectra for various quasi-0D structures measured at 10 K, together with that of a strained SQW of $In_{0.52}Ga_{0.48}As/GaAs$ for comparison. The spectrum of the unphosphidated dots shows 20 or more fine peaks, which should be attributed to 0D-confined excitons in the individual dots located within the effective probe aperture (approximately 300 nm, estimated by a line-scan profile). From the area-density of the dots, approximately 40 dots are expected within a 300 nm diameter. In a macroscopic PL measurement, the peak energy of 1.287 eV and the full-width at half maximum (FWHM) of 70 meV were obtained for the unphosphidated dots. The near-field PL spectrum has a slightly higher energy and a

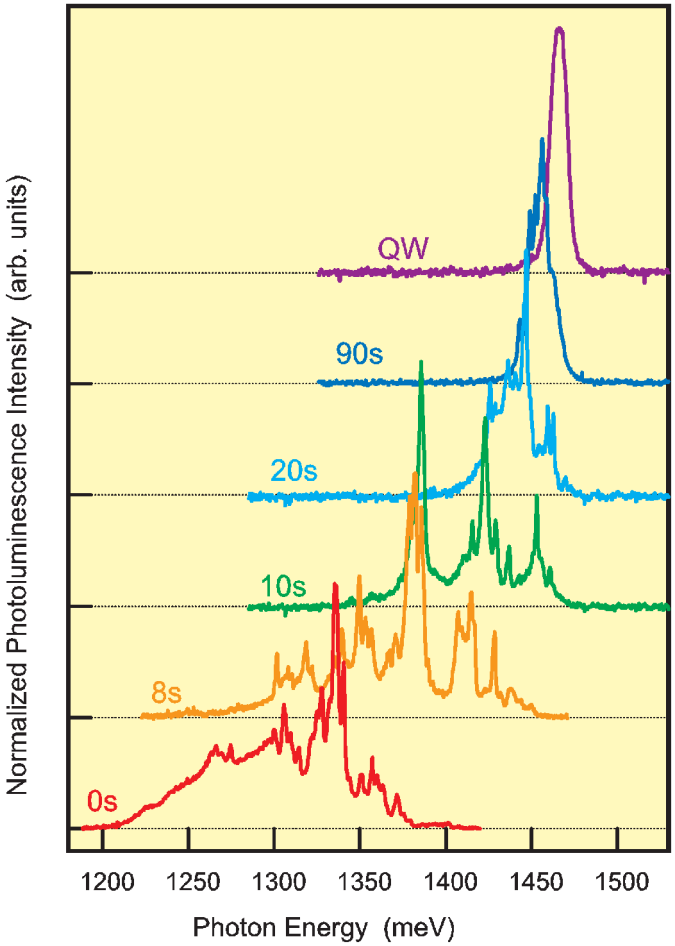

Fig. 3. Near-field PL spectrum of dots with various degrees of phosphidation measured at 10 K. Spectrum of strained InGaAs QW is also presented for comparison.

larger distribution for the envelope spectrum compared to the macroscopic measurement. As phosphidation time increased, the distributed fine peaks converged into one broad peak, as expected by the transition of 0D $\rightarrow$ 2D, with shifting of the spectrum centre to a higher energy due to the increase in the energy gap of QDs (InGaAs $\rightarrow$ InGaAsP, Fig. 1). The peak energy and FWHM of the macroscopic PL spectrum of the 90 s-phosphidated structure were 1.442 eV and 15 meV, respectively, while they are 1.455 eV and 13 meV in the near-field PL spectrum. We attributed the difference between the macroscopic and microscopic PL measuremens to the areal nonuniformity and probe-induced pressure effects, as discussed later.

In the process of 0D $\rightarrow$ 2D transition, the coexistence of 0D and 2D confinement occurs, as shown by the fine peaks superimposed on the QW broad peak in the spectrum of 20 s-phosphidated dots. It is worth noting that the photon energies of 0D peaks and the merged QW peak are almost the same as seen in the spectrum for 20 or 90 s-phosphidated structures. In the strain-induced QD superlattice on a multi-quantum-well (MQW) or InAs QDs densely formed on a GaAs(311)B surface, a red shift such as of 20–50 meV due to the dot-to-dot electron interaction has been reported [14–16]. Compared to that, no significant red shift was observed between fine 0D peaks and the merged QW peak for 20 or 90 s-phosphidated structures,

indicating that the excitons in the quasi-0D confinement studied here are isolated from each other even when the dots fuse into a layer. The small fine peaks in the spectrum of the 90 s-phosphidated structure indicate the existence of residual 0D confinement in the 2D layer formed by the coalescence of the dots. The residual 0D confinement is distinct in the lower energy side of the QW peak, indicating that the origin of 0D confinement should be the undulation of the QW layer [10]. The widths of the fine peaks in the spectrum for the 0 to 90 s-phosphidated structures are in the range of 0.5–1.4 meV, and show little dependence on phosphidation time. These observations show that there remain some less-phosphidated QDs in the quasi-0D structures which are spatially isolated residual 0D-confinements with distinctive QD levels at the lower energies.

3.2. Pressure effects on near-field PL

Differences between conventional 0D confinement and quasi-0D confinement should appear when an external perturbation such as strain or an electric field is applied. The perturbation brings about the emission of excitons weakly confined in 0D potentials into the 2D conduction layer. The pressure effects are especially important and informative, since pressure causes an increase in the energy gaps of 0D potentials and barriers, as well as Γ–X crossover at high pressures. In our experiments, the pressure effects on near-field PL spectra were observed by pressing the probe down on the sample.

The pressure–spectrum diagrams of the near-field photoluminescence are given in Fig. 4A and B. In the diagrams, the pressure is referred to as probe Z-motion, which is the nominal distance of the probe pressing down on the surface, since it is difficult to determine the actual localized pressure [17]. The nominal distance was obtained from the voltage applied to the probe-driving piezo-unit. It should be noted that the spectra in the diagrams were reproducible for the probe movements, i.e. the change of the spectrum could be traced back by driving the probe backward. This indicates that the probe movement induced the elastic deformation of the sample but destroyed neither the probe nor the sample. For the first approximation, we treat the probe-induced pressure as uniaxial stress localized at the contact area under the probe. This approximation is reasonable since the luminescence originated at a certain depth (50 nm from the surface, at the level of QDs) that is much smaller than the nominal diameter of the probe (approximately 2–3 μm), and only the luminescence from a small area beneath the probe was detected through the effective probe aperture (approximately 300 nm).

For the unphosphidated dots, the pressure increase causes blue shifts of the fine peaks over 100 meV. The large blue shifts are due to the compressive uniaxial strain, which enlarges the energy gaps of QDs as reported in references [18–20]. The piezoelectric effects are known to be negligible for InAs/GaAs QDs [21]. The blue shift of 100 meV in the InGaAs/GaAs dots corresponds to approximately 12 kbar of the applied pressure, with a pressure coefficient of 8–9 meV kbar^{-2} reported by static three-dimensional (3D) pressure experiments [19]. For the uniaxial compressive strain ($\varepsilon_{zz} > 0$) induced by pressure (P_{zz}) with the condition of zero stress in the x- and y-direction ($P_{xx} = P_{yy} = 0$), the strain (ε_{xx}, ε_{yy}, ε_{zz}) and the pressure are related as

$$\varepsilon_{xx} = \varepsilon_{yy} = -C_{12}/(C_{11} + C_{12})\varepsilon_{zz}, \tag{1}$$

$$P_{zz} = C_{12}(\varepsilon_{xx} + \varepsilon_{yy}) + C_{11}\varepsilon_{zz}. \tag{2}$$

Then the hydrostatic component (ΔE_{hyd}) and shear component (ΔE_{shr}) of the band-gap increase are given by

$$\Delta E_{\mathrm{hyd}} = -A(C_{11} - C_{12})/(C_{11} + C_{12})\varepsilon_{zz}, \tag{3}$$

$$\Delta E_{\mathrm{shr}} = B(C_{11} + C_{12})/(C_{11} + C_{12})\varepsilon_{zz}, \tag{4}$$

where A and B are the hydrostatic and shear deformation potentials, the Cs are elastic constants [22–25]. Concerning light-hold-related transition essential for the compressive strain, the total band-gap increase (ΔE_{tot}) is therefore

$$\Delta E_{\mathrm{tot}} = \Delta E_{\mathrm{hyd}} + \Delta E_{\mathrm{shr}}. \tag{5}$$

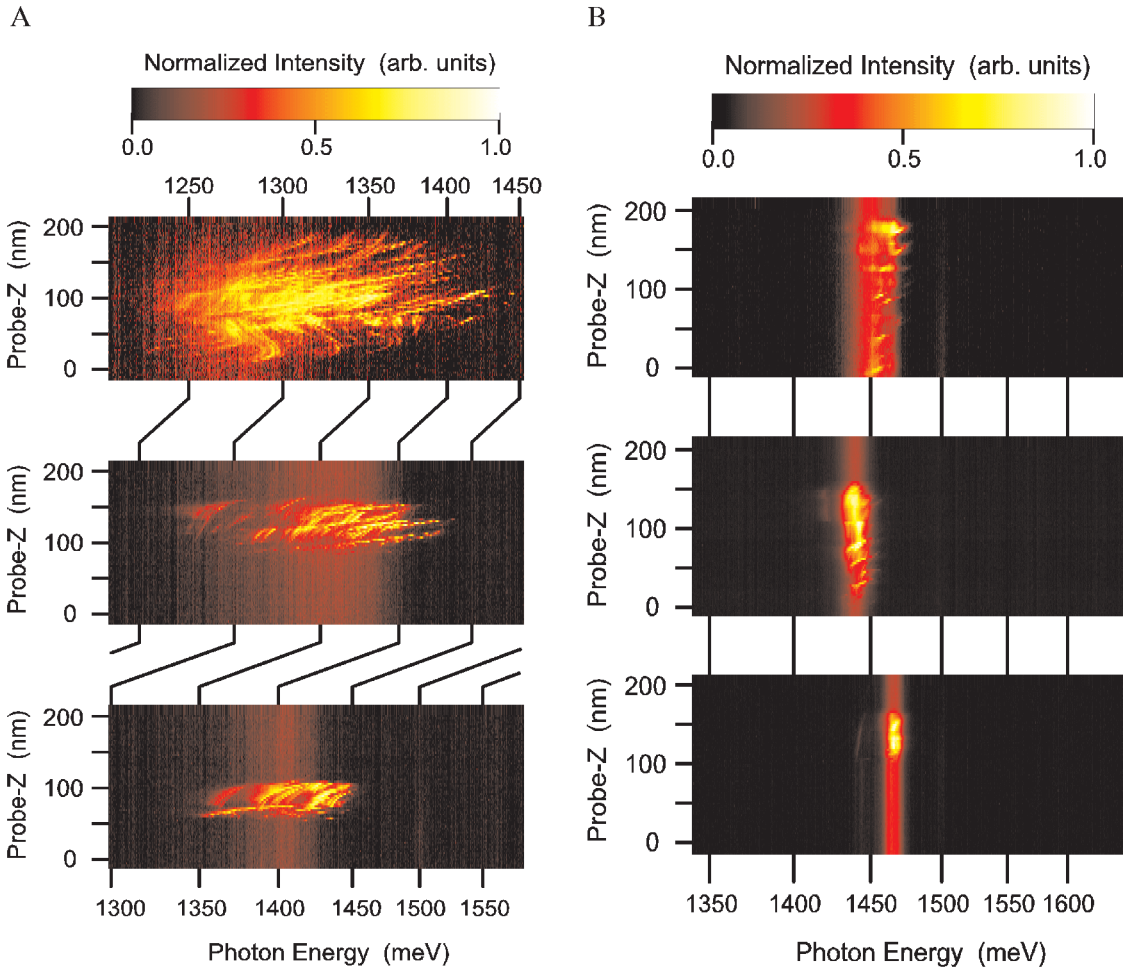

Fig. 4. Pressure dependence of nanoprobe PL spectrum observed as probe Z-motion dependence (see text). A, phosphidation time 0s (top), 8s (middle), 10s (bottom) and; B, 20 s (top), 90 s (middle), QW for comparison (bottom). Intensity in each diagram is normalized.

On the other hand, for the pressure P_{zz} with the condition of zero strain in the x- and y-direction ($\varepsilon_{xx} = \varepsilon_{yy} = 0$), the band-gap increase should be simply

$$\Delta E_{\text{tot}} = \Delta E_{\text{hyd}} = -A\varepsilon_{zz}. \tag{6}$$

By using the parameters for $In_{0.5}Ga_{0.5}As$ bulk, which are $C_{11} = 10.07 \times 10^{11}$ dyn cm^{-2}, $C_{12} = 4.93 \times 10^{11}$ dyn cm^{-2}, $A = -7.35$ eV, and $B = -1.75$ eV [24], respectively, we can evaluate the pressure P_{zz} necessary to cause the blue shift of 100 meV, for each case of $P_{xx} = P_{yy} = 0$ or $\varepsilon_{xx} = \varepsilon_{yy} = 0$. A reasonable value of $P_{zz} = 13.7$ kbar was obtained with eqn (6), while $P_{zz} = 430$ kbar calculated with eqn (5) was far beyond the reports [19]. This evaluation indicates that probe-induced pressure in this study can be treated as a uniform uniaxial pressure without shear component for the dots measured, since the probe aperture is much larger than the diameter of the dots.

By further pressure increase, the fine peaks in Fig. 4A disappeared after blue shift over 100 meV. However, there is no obvious evidence in the diagram of unphosphidated dots that the Γ–X crossover takes place, since

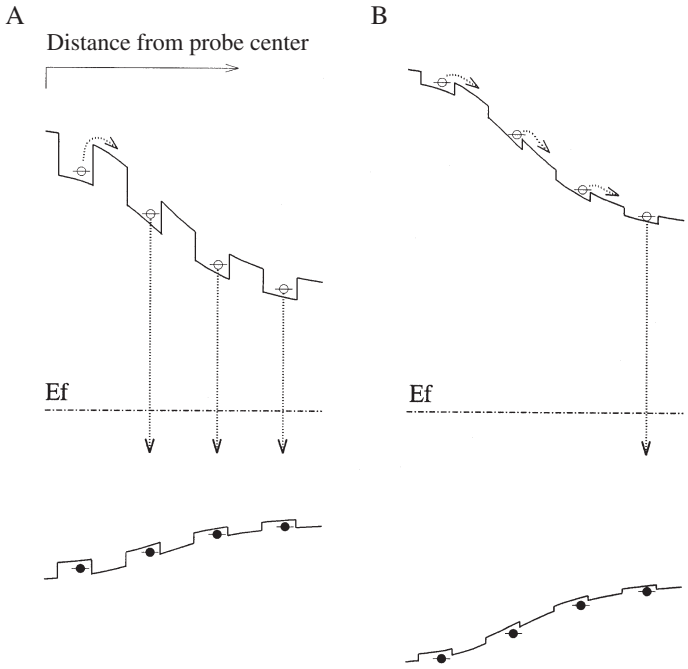

Fig. 5. Schematic diagram of energy band under probe-induced pressure for A, deep 0D confinement with immobile excitons and; B, shallow 0D potential where excitons diffuse along band slope.

almost all the peaks disappeared without showing any red shift at higher pressures. A few peaks showed small red/blue shifts at lower pressures (Fig. 4A, top), but these should be attributed to the instability of probe-induced pressure at the beginning of probe-surface contact. Itskevich *et al*. [19] observed the Γ–X crossover at 50 kbar of static 3D pressure in a macroscopic PL measurement of an InAs/GaAs QD system. They concluded that there is type-II alignment for X-valley-related states, i.e. the crossover corresponds to an intersection of the energies of the size-quantized Γ states in the InAs QDs and X-valley free-electron states in the bulk GaAs matrix. Compared to that used in their experiments, the estimated pressure of 12 kbar for the disappearance of fine PL peaks is too low for the crossover, even if the dimensionality of the applied pressure differs as localized 0D and static 3D. As discussed later, the disappearance can be explained by the exciton emission to the mobile carriers in the 2D layer.

The fine peaks for 8 and 10 s-phosphidated dots shift to blue with the applied pressure as do those for unphosphidated dots, though the shifts are rather small and the pressure range where the peaks are observed is limited. It is not clear at this moment why the pressure range is limited for 8 and 10 s-phosphidated dots. For the structures with 20 and 90 s-phosphidation, only small numbers of the fine peaks appear at very restricted photon energies close to the converged QW peak. The small blue shifts of fine peaks for the 20 and 90 s-phosphidated structures are approximately 15 meV at most, which corresponds to 1.8 kbar. Moreover, the broad QW peak in the diagrams for 20 and 90 s-phosphidated structures showed no shift with the pressure. The applied pressure should increase the energy gap of the QW layer as well as that of the QDs, and therefore should cause similar blue shifts both for the QW peak and the 0D fine peaks. The result obtained suggests that the luminescence observed comes from an unstrained QW, and that the carrier diffusion must be considered to determine the probe-induced pressure effects.

We consider that phote-induced carriers diffuse laterally in the QW layer due to a lateral pressure gradient along the radial axis of the probe. As shown in Fig. 5, the pressure gradient evoked by the apex of the probe

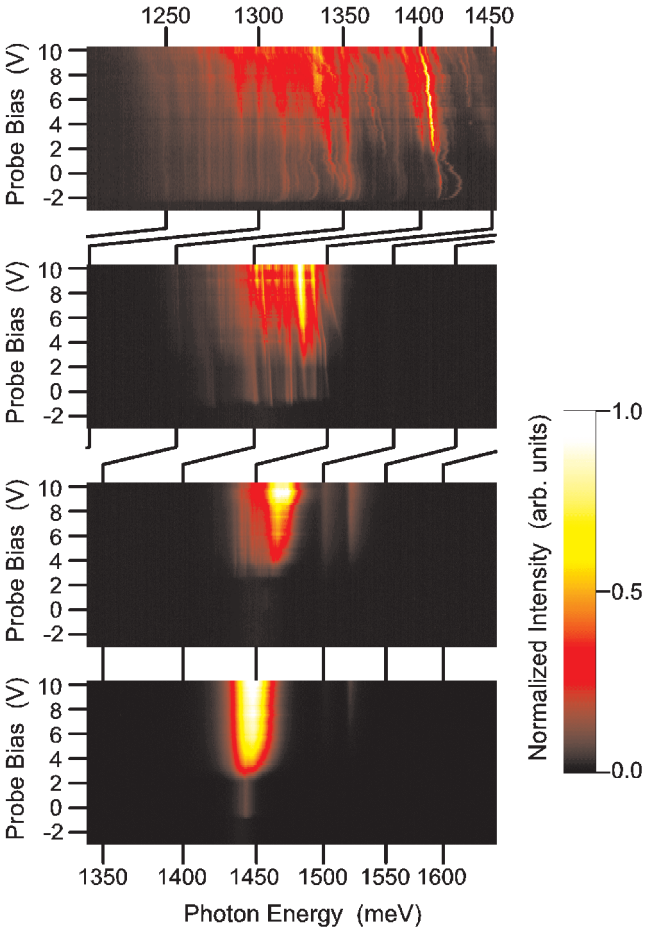

Fig. 6. Probe-bias dependence of nanoprobe PL spectrum for phosphidation times 0, 10, 20 and 90 s (from top to bottom). Intensity in each diagram is normalized.

generates a slope of the energy gap. When the 0D potentials are sufficiently deep, the excitons in QDs are still confined in 0D potentials even with the energy-gap gradient. The 0D potentials in unphosphidated QDs are 180 meV deep ($\triangle$ Ec + $\triangle$ Ev), as estimated from the difference in low-temperature PL peak energy between QDs and a wetting layer (233 meV difference between QDs and the GaAs barrier). Due to the large potential barrier, the excitons in the 0D potential were immobile against the energy-gap gradient for the quasi-0D confinements in 0–10 s phosphidated structures (Fig. 5A), as long as the pressure does not exceed 12 kbar, where the disappearance of fine PL peaks was observed. Above 12 kbar, the excitons are emitted into the QW layer (or wetting layer) by thermal excitation and by tunneling through the barrier slope (we estimate from a line-scan profile that the slope of the energy gap reaches up to 2.4 V/μm at 12 kbar). The emitted carriers in the 2D layer diffuse along the energy-gap gradient, and escape the detection limit of the effective probe aperture. As well, the diffusion of photoinduced carriers into the detection area is prevented by the energy-gap slope.

When the 0D potentials become shallow by further phosphidation over 10 s, the excitons in weak 0D potentials start to deplete and diffuse along the energy-gap gradient with much smaller pressures such as 1.8 kbar (Fig. 5B), resulting in the disappearance of fine 0D peaks at a small blue shift. On the other hand,

the carriers in the QW layer diffuse with any slight energy-gap gradient to the area without pressure, i.e. out of the effective aperture. Therefore, the QW peak does not shift at all with the applied pressures, but disappears when the entire effective detection area is affected by the pressure. This explanation can account reasonably well for the large blue shift observed for 0 and 10 s-phosphidated dots as well as the small blue shift of fine 0D peaks and the lack of shift of the QW peak for 20 and 90 s-phosphidated structures. The results also indicate that the excitons in the quasi-0D confinements (e.g. 20 or 90 s-phosphidated structures with the coexistence of 0D and 2D confinement in the same layer) can be excited and become mobile with small external perturbations comparable to 20–30 meV.

3.3. Bias effects on near-field PL

A large difference is expected in the mobility of carriers between completely-0D confinement and quasi-0D confinement, since the coexisting 2D layer in quasi-0D structures should contribute to the carrier diffusion when an electric field is applied. In our near-field PL measurement, the electric field can be generated by applying a bias to the Au-coated probe. It is difficult to determine the accurate profile of the electric field around the probe, but it is reasonable to assume that the profile is semispherical beneath the probe.

Figure 6 shows the near-field PL diagrams with the change in the probe bias. A small probe induced pressure such as approximately 5 kbar was applied to ensure the probe contact on the surface. For the unphosphidated structure, an increase by a factor of 5.9 in PL peak intensity was observed together with a small red shift of 8–9 meV when the probe bias was increased from 0 V to +10 V. The PL peak intensity becomes larger with increasing phosphidation time. For 20 s-phosphidated dots, the broad QW peak was increased by more than one order of magnitude (49.5) when the positive probe-bias of up to +10 V was applied. The difference in the increase of the PL peak indicates that the effective attraction of photoinduced carriers (electrons) toward the probe occurred through the 2D conductive layer formed by the coalescence of the dots. Note that the positive bias should be repulsive to the photogenerated holes. We believe that the hole diffusion induced by the electric field is rather small and contributes less to the bias-dependence compared to that of electrons due to the larger effective mass and the lower mobility of holes. The red shifts of the fine PL peaks observed for 0 and 10 s-phosphidated structures are caused by the quantum-confined Stark effects for 0D confinements [26–28]. Energy shifts of fine peaks were not observable for 20 and 90 s-phosphidated structures since the QW peak grew significantly and hid the fine peaks.

The confinement of excitons in 0D potentials and the diffusion/conduction of carriers in 2D layers are in a trade-off relationship for quasi-0D confinements, and can be controlled by adjusting the phosphidation time for the quasi-0D system prepared in this study.

4. Conclusions

We have demonstrated the probe-induced pressure effects and the probe-bias effects on the near-field nanoprobe photoluminescence for quasi-0D confinement structures of InGaAs(P)/GaAs with various degrees of 0D/2D. The coexistence of 0D and 2D confinement was proven by the fine PL peaks of 0D confinement superimposed on the QW peak. Large blue shifts with increase in pressure were observed for 0D fine PL peaks but not for the QW peak. The disappearance of fine 0D peaks due to larger probe-induced pressures should be attributed to carrier diffusion rather than to Γ–X crossover. The QW peak was increased by more than one order of magnitude with the positive probe bias up to +10 V, while 0D fine PL peaks showed smaller increases up to 5.9 with red shifts of 8–9 meV. These results can be explained by the coexistence of immobile excitons in 0D potentials and mobile carriers in the 2D (QW) layer; with external perturbation such as pressure or electric field, the excitons weakly confined in 0D potentials are emitted to the 2D conductive layer and diffuse according to the energy-gap gradient or the electric field. The quasi-0D confinement will be useful for various applications including nanosensors, where external perturbation is detected through conduction change in a 2D layer caused by emission of immobile excitons in 0D to the coexisting 2D conductive layer.

Acknowledgements—The authors acknowledge financial support from the Special Coordination Funds of the Ministry of Education, Culture, Sports, Science and Technology and the Japanese Government.

References

[1] G. Yusa and H. Sakaki, Physica **E2**, 734 (1988).
[2] A. J. Shields, M. O. O' Sullivan, I. Farrer, D. A. Ritchie, K. Cooper, C. L. Foden, and M. Pepper, Appl. Phys. Lett. **74**, 735 (1999).
[3] P. Dong, E. Towe, and S. Kennerly, Appl. Phys. Lett. **75**, 2719 (1999).
[4] S.-W. Lee, K. Hirakawa, and Y. Shimada, Physica **E7**, 499 (2000).
[5] G. Yusa and H. Sakaki, Superlatt. Microstruct. **25**, 247 (1999).
[6] W. V. Schoenfeld, T. Lundstrom, P. M. Petroff, and D. Gershoni, Appl. Phys. Lett. **74**, 2194 (1999).
[7] A. J. Shields, M. P. O' Sullivan, I. Farrer, C. E. Norman, D. A. Ritchie, K. Cooper, and M. Pepper, Physica **E7**, 479 (2000).
[8] D. Heinrich, J. Hoffmann, J. J. Finley, A. Zrenner, G. Bohm, and G. Abstreiter, Physica **E7**, 484 (2000).
[9] H. Kim, T. Noda, T. Kawazu, and H. Sakaki, Japan. J. Appl. Phys. **39**, 7100 (2000).
[10] K. Ozasa, Y. Aoyagi, Y. J. Park, and L. Samuelson, Appl. Phys. Lett. **71**, 797 (1997).
[11] K. Ozasa and Y. Aoyagi, J. Cryst. Growth **188**, 370 (1998).
[12] K. Ozasa and Y. Aoyagi, J. Electron. Mater. **28**, 437 (1999).
[13] K. Ozasa, S. Nomura, M. Takeuchi, and Y. Aoyagi, Mater. Sci. Eng. **B86**, 34 (2001).
[14] M. Sopanen, H. Lipsanen, J. Tulkki, and J. Ahopelto, Physica **E2**, 19 (1998).
[15] K. Akahane, S. Lan, T. Kawamura, T. Takamasu, G. Kido, Y. Okada, and M. Kawabe, Japan. J. Appl. Phys. **39**, 1100 (2000).
[16] S. Fafard, M. Spanner, J. P. McCaffrey, and Z. R. Wasilewski, Appl. Phys. Lett. **76**, 2268 (2000).
[17] A. Chavez-Pirson, J. Temmyo, and H. Ando, Physica **E7**, 367 (2000).
[18] J. L. Sly and D. J. Dunstan, Phys. Rev. **B53**, 10116 (1996).
[19] I. E. Itskevich, S. G. Lyapin, I. A. Troyan, P. C. Klipstein, L. Eaves, P. C. Main, and M. Henini, Phys. Rev. **B58**, R4250 (1998).
[20] J. Phillips, P. Bhattacharya, and U. Venkateswaran, Appl. Phys. Lett. **74**, 1549 (1999).
[21] M. Grundmann, O. Stier, and D. Bimberg, Phys. Rev. **B52**, 11969 (1995).
[22] A. Gavini and M. Cardona, Phys. Rev. **B1**, 672 (1970).
[23] H. Asai and K. Oe, J. Appl. Phys. **54**, 2052 (1983).
[24] B. A. Foreman, Phys. Rev. **B49**, 1757 (1994).
[25] E. M. Goldys and J. J. Shi, Phys. Status. Solidi. **B210**, 237 (1998).
[26] Y. P. Feng and H. N. Spector, Phys. Rev. **B48**, 1963 (1993).
[27] M.-E. Pistol, D. Hessman, J. Lindahl, L. Montelius, and L. Samuelson, Mater. Sci. Eng. **B42**, 82 (1996).
[28] M. S. Skolnick, I. E. Itskevich, P. W. Fry *et al*., Physica **E6**, 348 (2000).